Turkish Journal of Electrical Engineering & Computer Sciences

http://journals.tubitak.gov.tr/elektrik/

Research Article

Turk J Elec Eng & Comp Sci
(2014) 22: 924 – 939

doi:10.3906/elk-1208-54

Fuzzy impedance and force control of a Stewart platform

Selçuk KİZİR*, Zafer BİNGÜL
Department of Mechatronics Engineering, Kocaeli University, Umuttepe Campus, Kocaeli, Turkey

Received: 15.08.2012 • **Accepted:** 21.01.2013 • **Published Online:** 17.06.2014 • **Printed:** 16.07.2014

Abstract: A new, simple, and effective control method is proposed for the position-based impedance and force control of a Stewart platform (SP). The control approach can be divided into 3 parts, namely position control in free space, impedance control in contact, and force control. An impedance filter is developed to achieve the desired behavior between the position and force. The gain of the filter is modified by a fuzzy logic proportional-integral-derivative controller. Kinematic and dynamic models of the SP are simulated in a MATLAB/Simulink environment. Several real-time experiments are conducted with the SP developed in our laboratory. The results of the simulations and real-time experiments are compared to show the effectiveness of the proposed method. The experimental results demonstrate that the position control of the SP in Cartesian space is achieved at up to precision of 0.5 μm and 0.43 μ° in linear and rotational motions, respectively, and force control of the SP is obtained successfully with a range of between 1 N and 50 N. Steady-state force errors are also eliminated with an intelligent integrator.

Key words: Impedance control, force control, fuzzy logic, Stewart platform, parallel manipulator

1. Introduction

The Stewart platform (SP) is the most widely used and well-known parallel type of manipulator. It was first developed by the Stewart and Gough as an aircraft simulator and tire testing mechanism [1]. The SP is a 6-degrees of freedom (DOF) mechanism controlled by 6 prismatic links that are connected between 2 plates, fixed and mobile. Parallel manipulators are frequently used in the field of medical robotics; simulators for airplanes, helicopters, and vehicles; satellite positioning systems; laser cutting systems; missile launch platforms; and precision manufacturing systems [2].

Fuzzy logic allows emulating human decision-making and reasoning based on if/then rules. The fuzzy set theory has been used in control engineering since it was first introduced in 1965 [3]. An inference system, which is the core structure of the fuzzy control system, consists of input and output membership functions, a knowledge base, fuzzification, an inference engine, and defuzzification. A fuzzy inference system provides nonlinear mapping between its input and output space.

Generally, robot control can be classified as position and force control. Although the position and trajectory control are the 2 main control tasks in robotic systems, force and interaction control with different environments (contact, collision) have also been widely studied. Force control is required for some tasks in robotic applications, such as grinding, deburring, polishing, assembly, contour-tracking, and surgery. Some fundamental methods for robot force control have been developed in the last two decades. These control methods

*Correspondence: selcuk.kizir@kocaeli.edu.tr

can be summarized as stiffness [4], impedance [5], admittance, hybrid position/force, hybrid impedance, parallel position/force, pure force control [6,7], and computed torque control [8]. In addition, some advanced methods have been developed such as fuzzy [9], adaptive [10], robust [11], vision based [12], and learning algorithms [13].

The impedance control method is used for the interaction between the robot-end effector and objects. The impedance method was proposed by Hogan [5] and aims to regulate the mechanical impedance between the robot and object. Impedance control has been applied in the literature as position-based and force-based. Position-based impedance control in robotic systems with a conventional position controller is suitable and reliable for the requirement of the force and interaction control [14].

In this study, a new, simple, and effective control method is proposed for the position based impedance/force control of the SP. The control objectives here can be divided into 3 parts: a) position control in free space, b) impedance control during contact interaction, and c) force control. Position control of the SP can be made in Cartesian or joint space. In order to have position control of the SP, forward and inverse kinematics are needed in Cartesian space and joint space, respectively. Contrary to serial robots, the inverse kinematics of the parallel manipulators is very simple relative to forward kinematics. Each leg in the SP is controlled by a servo position regulator. The mechanical impedance between a robot and an object is defined by a second-order mass-spring-damper system. This relationship can be defined as an impedance filter between the force and robot position. The gain of the filter is adjusted by a fuzzy logic controller. As interaction occurs, force control is achieved by the fuzzy controller. There are not many studies about impedance and force control of the SP in the literature. Most of the studies in the literature have focused on serial robots rather than parallel robots. Ömürlü and Yıldız [4] presented experimental results comparing the various controller structures about the control of a 3 $\times$ 3 SP with a force/torque feedback. They showed that parallel-connected self-tuning fuzzy PD and PD controllers have better performance than independent PD, fuzzy PD and self-tuning fuzzy PD controllers. Davliakos and Papadopoulos [15] proposed a torque-based impedance controller in joint space for model-based impedance control of an electro-hydraulic SP. They showed that the impedance control method gives better performance than PD controllers for interaction control by simulations. They designed the impedance control method in joint space and so forward kinematics, which is a difficult problem for parallel manipulators, was not used. However, their work was only for interaction control rather than force control.

In the next sections of the paper, the experimental SP system used in this study will be described; the kinematics and dynamics of the SP will be given and the fuzzy impedance/force control method and controller design will be presented. Finally, simulation and experimental results will be summarized.

2. SP system

The experimental system used for this study consists of 2 main bodies (mobile and fixed plates), 6 linear joints, a real-time controller, a 6-DOF mouse (space navigator), a 6-DOF haptic device (phantom omni) with a 3-DOF force feedback, a 6-DOF force-torque sensor (ATI-gamma), power supply, emergency stop circuit, and an interface board. The control algorithms developed here are embedded in a Dspace DS1103 real-time controller. Figure 1 shows the SP system and force test apparatus.

3. Kinematic and dynamic modeling of the SP

A robot model consists of some mathematical expressions, such as forward and inverse kinematics, Jacobian, and dynamics. These equations are defined in the rest of the section. They will be used for the simulation and real-time control.

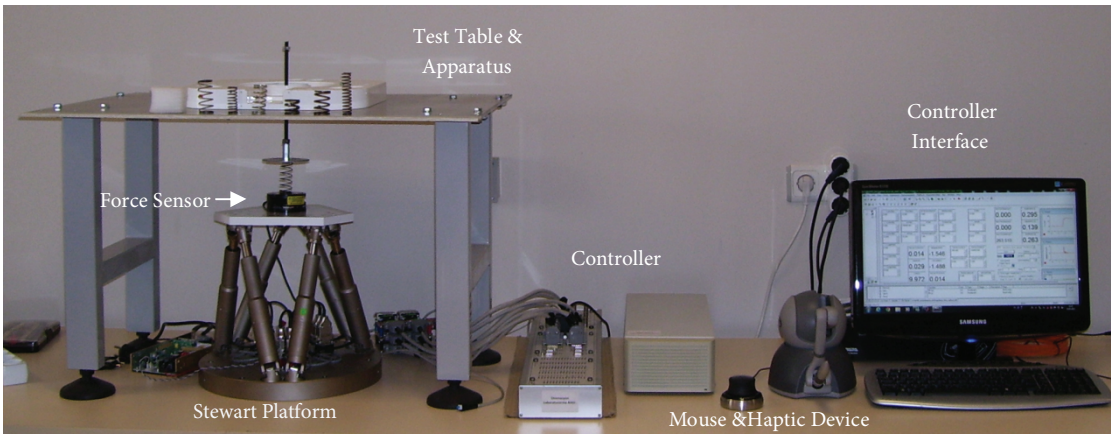

Figure 1. SP system and impedance/force control test setup.

Robot kinematics is a set of expressions defining the geometric relationships of the robot between joint space and Cartesian space. In order to find the inverse kinematics relation of the SP, coordinate systems are placed as shown in Figure 2. The $B = \{X,\ Y,\ Z\}$ and $T = \{x,\ y,\ z\}$ main coordinate systems are fixed at the center of the base plate and upper mobile plate. The $\mathbf{B_i}$ $(i = 1, 2, .. 6)$ and $\mathbf{T_i}$ $(i = 1, 2, .. 6)$ joint coordinate systems are placed on the lower and upper centers of the joints.

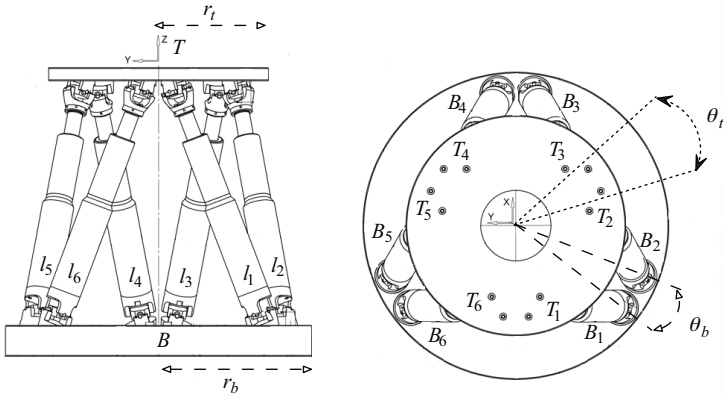

Figure 2. SP structure and coordinate systems.

The base and top joint coordinates can be expressed as:

$$\mathbf{T_i} = \begin{bmatrix} T_{ix} \\ T_{iy} \\ T_{iz} \end{bmatrix} = \begin{bmatrix} r_t cos(\lambda_i) \\ r_t sin(\lambda_i) \\ 0 \end{bmatrix}, \tag{1}$$

$$\lambda_i = \frac{i\pi}{3} - \frac{\theta_t}{2} \quad i = 1,\ 3,\ 5, \tag{2}$$

$$\lambda_i = \lambda_{i-1} + \theta_t \quad i = 2,\ 4,\ 6, \tag{3}$$

$$\mathbf{B_i} = \begin{bmatrix} B_{ix} \\ B_{iy} \\ B_{iz} \end{bmatrix} = \begin{bmatrix} r_b cos(\nu_i) \\ r_b sin(\nu_i) \\ 0 \end{bmatrix}, \tag{4}$$

$$\nu_i = \frac{i\pi}{3} - \frac{\theta_b}{2} \quad i= 1,\ 3,\ 5, \tag{5}$$

$$\nu_i = \nu_{i-1} + \theta_b \quad i= 2,\ 4,\ 6, \tag{6}$$

where r_t and r_b are the radius of the top and base plates and θ_t and θ_b are the angles between the connection points of the upper and lower plates, respectively.

Given the position vector $\mathbf{P}$ and the orientation matrix $\mathbf{R}$, the leg lengths to drive the robot to its desired position and orientation according to a fixed plate can be computed from the following equation:

$$\mathbf{L_i}=\mathbf{R_{XYZ}T_i}+\mathbf{P}-\mathbf{B_i} i = 1, 2, \ldots, 6. \tag{7}$$

Finally, the norm of the vectors ($\mathbf{L_i}$) are the desired leg lengths ($l_i= \|\mathbf{L_i}\|$). $\mathbf{P}=[P_X P_Y P_Z]$ is the desired position to be reached in free space according to the $B = \{X,\ Y,\ Z\}$ coordinate system in the equation.

In the SP, another important topic aside from kinematics is the Jacobian matrix. The Jacobian can be defined as in the following equations:

$$\dot{L}= \mathbf{J}\dot{X}, \tag{8}$$

$$\tau =\mathbf{J^T F}, \tag{9}$$

where $\dot{\mathbf{L}}$, $\dot{\mathbf{X}}$, $\boldsymbol{\tau}$, and $\mathbf{F}$ represent the leg velocity vector, end effector velocities, joint torques, and force applied to the actuators, respectively.

The dynamic model of the SP describes the relationship between the mobile platform and leg behavior in a mathematical form. This relationship can be defined in 2 different ways: forward and inverse. In the forward dynamics, the equation of motion describes how the upper plate (acceleration and speed) moves under the given joint torques/forces. On the other hand, the equations of the inverse dynamics define the required joint torques or forces to follow a reference trajectory.

The forward dynamics of an n-DOF manipulator are expressed by the following equation in Cartesian space [16]:

$$\mathbf{M}(\mathbf{X})\ddot{X}+\mathbf{C}\left(\mathbf{X},\dot{X}\right)\dot{X}+\mathbf{G}(\mathbf{X})=\mathbf{J^{-T}}\tau-\mathbf{F_e}, \tag{10}$$

where $\mathbf{M}$ is an 6×6 symmetric and positive definite inertia matrix, $\mathbf{C}$ is a coriolis and centripetal matrix, $\mathbf{G}$ is gravitational vector, $\boldsymbol{\tau}$ is the applied torque vector, $\mathbf{J}$ is the Jacobian matrix, $\mathbf{F}_e$ is the external forces, and $\mathbf{X}$ represents the position and orientation of the upper plate, respectively.

In order to obtain a full model of the system, actuator dynamics should be included in the SP model. A DC motor as a leg actuator can be defined below:

$$L_a\frac{di_a}{dt} + R_a i_a = V_a - K_b\dot{\theta}, \tag{11}$$

$$\tau_m - \tau_l = J_m\ddot{\theta} + B_m\dot{\theta}, \tag{12}$$

where θ is the rotor position (rad), τ_m is the motor torque (Nm), τ_l is the load torque, V_a is the input voltage (V), L_a is the inductance (H), R_a is the resistance (Ω), i_a is the armature current (A), K_b is the back EMF constant (V/rpm), J_m is the total inertia (Kgm^2), and B_m is the total damping (Nms/rad), respectively. Eq. (12) can be rewritten in matrix form as follows:

$$\tau_{\mathbf{m}}=\mathbf{M_a}\ddot{L}+\mathbf{N_a}\dot{L}+\mathbf{K_a}Y, \tag{13}$$

where $\mathbf{M_a} = \frac{2\pi}{p}(J_m)\mathbf{I_{6x6}}$, $\mathbf{N_a} = \frac{2\pi}{p}(B_m)\mathbf{I}_{6x6}$, $\mathbf{K_a} = \frac{p}{2\pi}\mathbf{I}_{6x6}$, $Y = \frac{2\pi}{p}\tau_l$, and p is the ball screw pitch.

Finally, the forward dynamics of the SP with actuator dynamics is obtained by [17]:

$$\tau_{\mathbf{m}} = \check{M}_{\mathbf{c}}\ddot{X} + \check{N}_{\mathbf{c}}\dot{X} + \check{G}_{\mathbf{c}}, \tag{14}$$

where

$$\check{M}_{\mathbf{c}} = \mathbf{M_a J} + \mathbf{K_a J^{-T} M}, \check{N}_{\mathbf{c}} = \mathbf{N_a J} + \mathbf{M_a}\dot{J} + \mathbf{K_a J^{-T} C},$$

and

$$\check{G}_{\mathbf{c}} = \mathbf{K_a J^{-T} G}.$$

The dynamic model of the SP with actuator dynamics shown in Figure 3 can be simulated using Eq. (14).

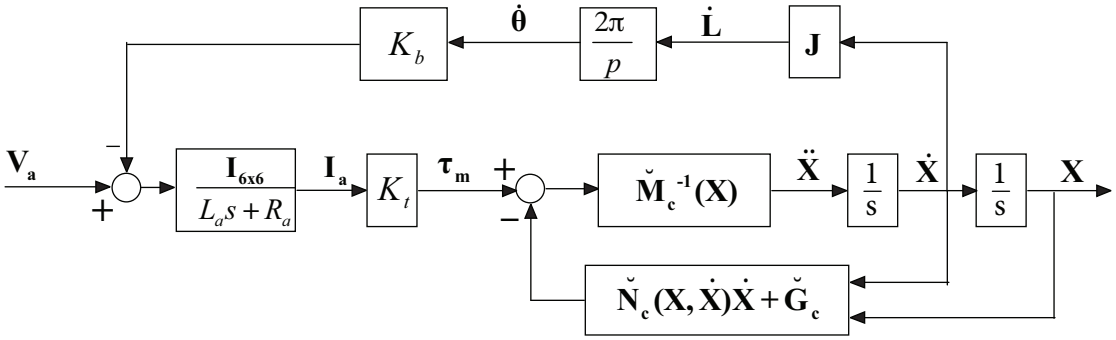

Figure 3. General block diagram of the SP dynamics.

4. Impedance control

The impedance control method developed by Hogan can be defined as an interaction control method rather than a force control method [5]. According to Hogan, the fundamental philosophy of impedance control is that the controller should be designed not only to track a motion trajectory alone, but also to regulate the mechanical impedance. The relation between the robot velocity and exerted force is called mechanical impedance.

The impedance control problem can be defined as a requirement of a controller design that resultant forces in contact will reveal a difference between the actual and reference positions of the robot based on the target impedance rule. Considering dynamics of the actuators and the system, the impedance control method can be designed based on position and force. In fact, impedance control is essentially based on position.

Design of the impedance control can be done using a zero-, first-, and second-order dynamic model, according to the force–motion relationship. As shown in Figure 4, mechanical impedance, which is expressed by a second-order mass-damper-spring system, is defined by the Eq. (15).

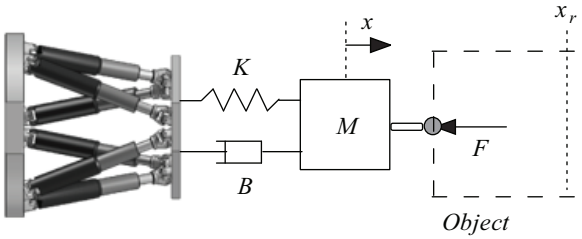

Figure 4. Virtual second-order mass-damper-spring system between a robot and object.

$$M\left(\ddot{x}-\ddot{x}_r\right)+B\left(\dot{x}-\dot{x}_r\right)+K\left(x-x_r\right)=F, \tag{15}$$

where M is the virtual mass, B is the virtual damping coefficient, K is the virtual spring constant, F is the force applied to the system, x is the real position, and x_r is the desired position of the virtual mass. Eq. (15) can be expressed in the frequency domain:

$$X(s)-X_r(s)=Z(s)F(s), \tag{16}$$

where $Z\left(s\right)=\frac{1}{Ms^2+Bs+K}$. The impedance filter ($Z(s)$) updates the position of the robot given by Eq. (16). The mechanical impedance determined by M, B, and K defines how the robot reacts to external forces acting during contact with an object. The impedance filter represents a well-known linear second-order system. The natural frequency and damping ratio of the second-order system are given below, respectively:

$$w_n=\sqrt{\frac{K}{M}}, \tag{17}$$

$$\xi=\frac{B}{2Mw_n}. \tag{18}$$

The stability of the position-based impedance control was studied and the stability conditions are found by Eq. (19), as below [9]:

$$\xi\geq 0.5(\sqrt{1+2k}-1), \tag{19}$$

where $k=K_e/K\gg 1$ and K_e is the stiffness of the environment or object. The desired stiffness K should be much smaller than the environment stiffness and the desired damping ratio should be high enough according to this criterion.

In the literature, the parameters (M, B, K) were determined in many different ways, such as varying these parameters with fuzzy logic controllers [9] and adaptive [10] or nonadaptive control strategies [15,18]. Moreover, the parameters are adjusted based on a switching mechanism [19].

In this study, the constant natural frequency and damping ratio is selected. The DC gain of the impedance filter is adjusted as the position and force control are applied to the SP. The damping ratio and natural frequency is set to 0.9 and 500 rad/s in order to decrease the system's response time and overshoot. The stiffness of the object should be higher than the determined value for the stability criteria. If a different desired interaction behavior is needed, these parameters can be adjusted based on the control requirement. In order to obtain the desired interaction behavior of the robot with different objects, the gain of impedance filter should be changed based on the external forces.

5. Controller design

The controller design can be divided into 3 parts: robot position control, impedance filter, and fuzzy impedance/force control. Figure 5 shows a general block diagram of the controller used here.

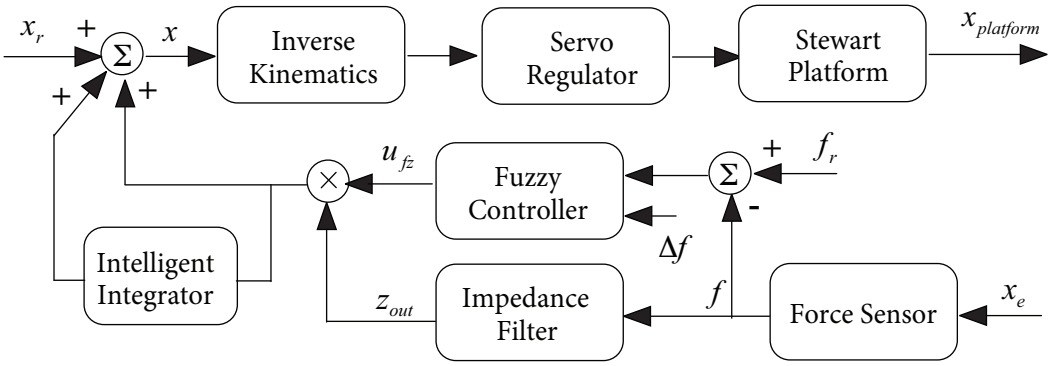

Figure 5. Block diagram of the fuzzy impedance/force controller.

Control output of the fuzzy/impedance controller can be defined by:

$$x = x_r + u_{fz}\left(f_r - f, \Delta f\right) z_{out} f K_f + K_{int} \int_{int}^{reset} \left(u_{fz}\left(f_r - f, \Delta f\right) z_{out} f K_f\right), \tag{20}$$

where x is the modified position, x_r is the desired position, f is the applied force, f_r is the desired force, Δf is the change in the force, z_{out} is the impedance filter output, u_{fz} is the fuzzy inference system output, K_f is the fuzzy output gain, and K_{int} is the integrator gain. The integrator in the equation also has a reset input and threshold limit.

5.1. Position control

Leg lengths are obtained from the inverse kinematics in Cartesian space. Position modifications, depending on the force/impedance controller, are controlled by a decentralized proportional-integral-derivative (PID) (servo regulator). The controller equation is given below and the controller structure is shown in Figure 6.

$$u = K_u \left[K_p e\left(t\right) - K_d \dot{l}\right] + K_i \int \left[K_p e\left(t\right) - K_d \dot{l}\right] \tag{21}$$

Controller parameters are optimized by the particle swarm optimization algorithm. A full SP dynamic model is used in Simulink in order to minimize the leg position errors under step and trajectory inputs, where the swarm size is selected as 10. The mean of root of squared error method is applied as a cost function. The controller parameters are determined as $K_p = 17.993$, $K_d = 0.0256$, $K_u = 1.0128$, and $K_i = 0.0255$.

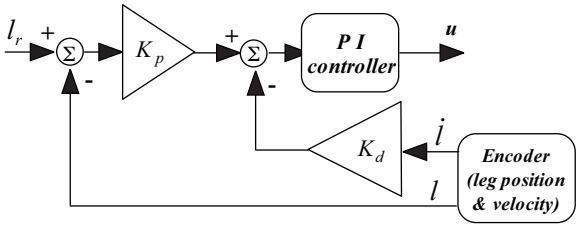

Figure 6. Leg servo controller.

5.2. Impedance filter

The filter equation is given below:

$$Z\left(s\right) = \frac{1}{s^2 + 900s + 250000} \tag{22}$$

Unit step and impulse responses of the filter are illustrated in Figure 7 to show natural behaviors of the impedance filter without any control action. As can be seen from the figure, the filter reaches the steady-state condition in 0.015 s.

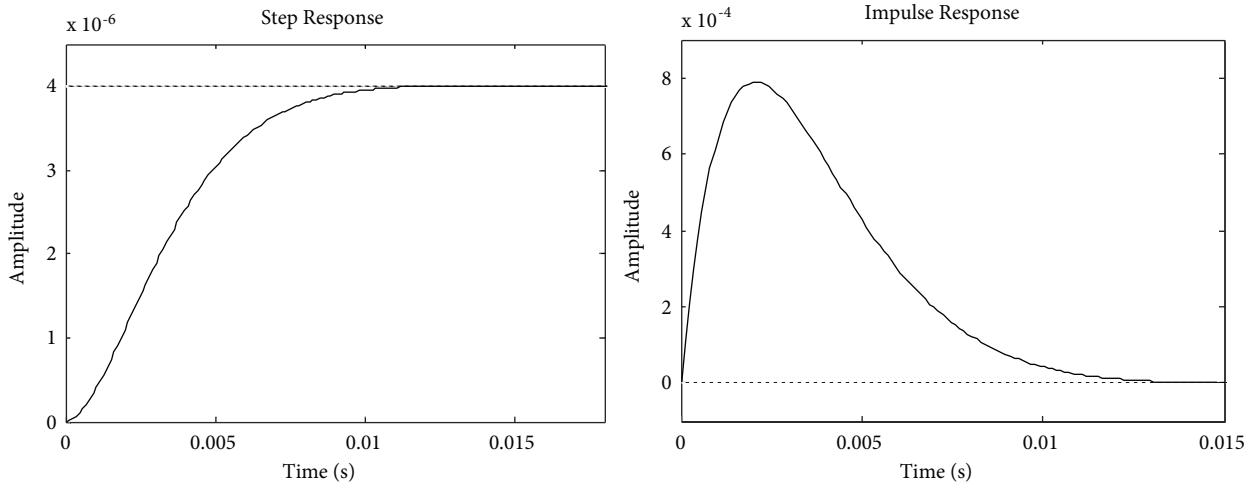

Figure 7. Filter responses.

5.3. Impedance/force control

Three main tasks are defined for the control of the SP:

1. Position control in free space
2. Impedance control in contact
3. Force control

As shown from the general control block diagram in Figure 5, the filter output will be 0, since $F = 0$ in free space, thus position control of the robot is provided. The fuzzy logic controller will adjust the impedance filter gain around the reference force if the robot is in contact with any surface. Next, the desired force is provided by the fuzzy PID controller. In order to eliminate the steady-state error, an integrator is added to the fuzzy PD controller. In order to prevent position modification, the integrator is enabled and reset, based on a force threshold. Position control in free space is provided even if a nonzero desired force input is given. Finally, a Mamdani Max-Min–type fuzzy logic controller is designed with 2 inputs and an output that has 7 membership functions with 49 rules. The force error and rate of force are inputs and the filter gain is the output of the fuzzy controller. Membership functions are chosen based on experiments using the simulation model and these functions are verified based on trial-and-error experiments. Rules are determined based on trial-and-error experiments to achieve the desired interaction in the contact moment and then the desired force. The rule base and membership functions are shown in Figure 8 and the Table.

6. Simulation and experimental results

The proposed controller is modeled in Simulink and applied to the SP system. Various simulations are conducted to test the validity of the proposed method. The force response and position change of the upper plate are shown in Figure 9. In this case, a 5-N force and 11-mm position in the z direction are applied as reference inputs. The stiffness of the object used here is 4700 N/m. The object is placed at 9 mm in the z-axis. As seen from Figure 9, the overshoot is only about 0.5 N in contact and the steady-state is then reached. In Figure

8, the range of membership functions is ± 50 N. As seen from Figure 8, the smallest controllable range (zero membership) is ± 1 N. The desired robot position, object position, robot position, and modified robot position (force controller output) are given in the right-hand side of Figure 8. The fuzzy force/impedance controller modifies the desired robot position after the interaction. As seen from the responses, the desired impedance force control is achieved in 0.1 s.

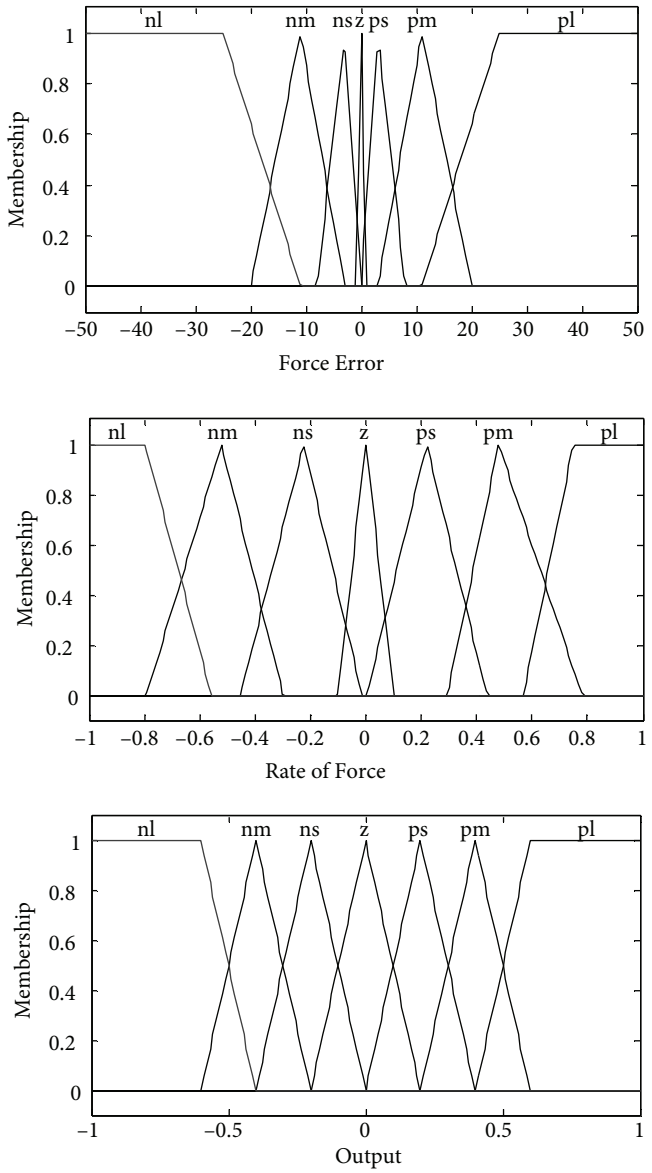

Figure 8. Input-output membership functions.

The system responses shown in Figure 10 are obtained with the same as conditions above, with reference inputs of 10-N force and 15-mm position. Although the reference inputs are changed, the dynamic behavior of the responses is not much different. The desired interaction between the robot and object is achieved and the interaction time is 0.3 s after the collision.

A real-time controller is designed in Simulink and embedded in Dspace 1103. The main controller model is shown in Figure 11. The model contains some subsystems. These are summarized as: force measurement

and force feedback submodel, haptic submodel, inverse kinematics and fuzzy impedance/force control model, leg position controller model, leg position measurement block, initialization routine, and output blocks.

Table. Rule base of the fuzzy/impedance controller.

		Rate of force						
		NL	NM	NS	Z	PS	PM	PL
Force error	NL	z	ns	nm	nl	nl	nl	nl
	NM	z	z	ns	nm	nl	nl	nl
	NS	z	z	z	ns	ns	nm	nl
	Z	pl	pm	ps	z	ns	nm	nl
	PS	pl	pm	ps	ps	z	z	z
	PM	pl	pl	pm	pm	ps	z	z
	PL	pl	pl	pl	pl	pm	ps	z

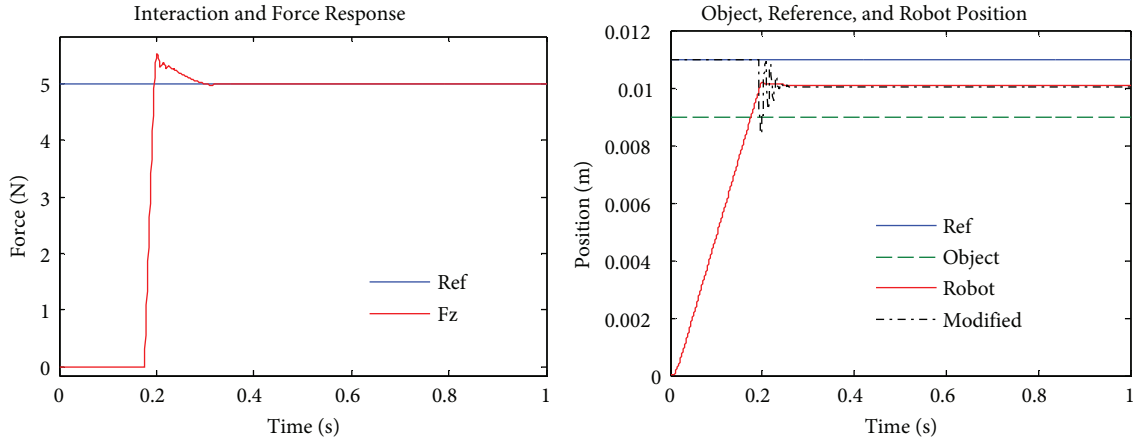

Figure 9. Simulation responses with reference inputs of 5-N force and 11-mm position in the z-axis.

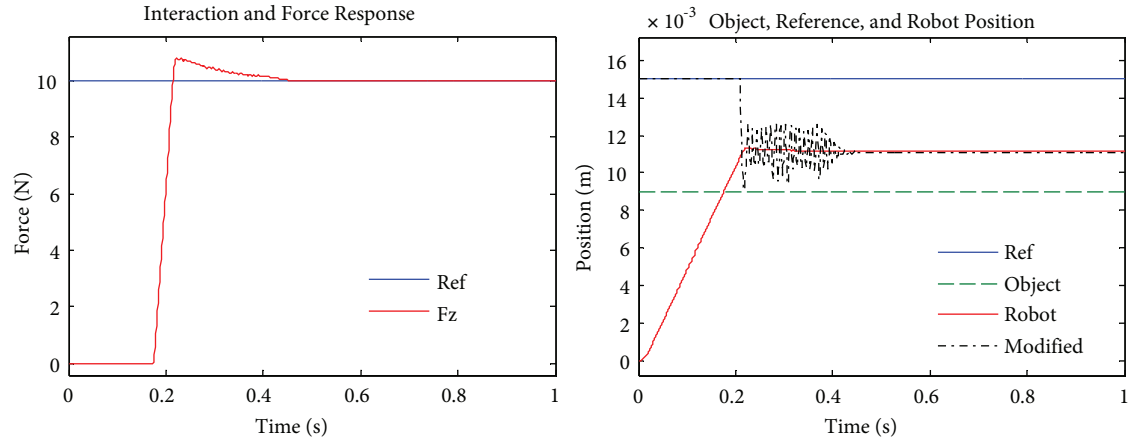

Figure 10. Simulation responses with reference inputs of 10-N force and 15-mm position in the z-axis.

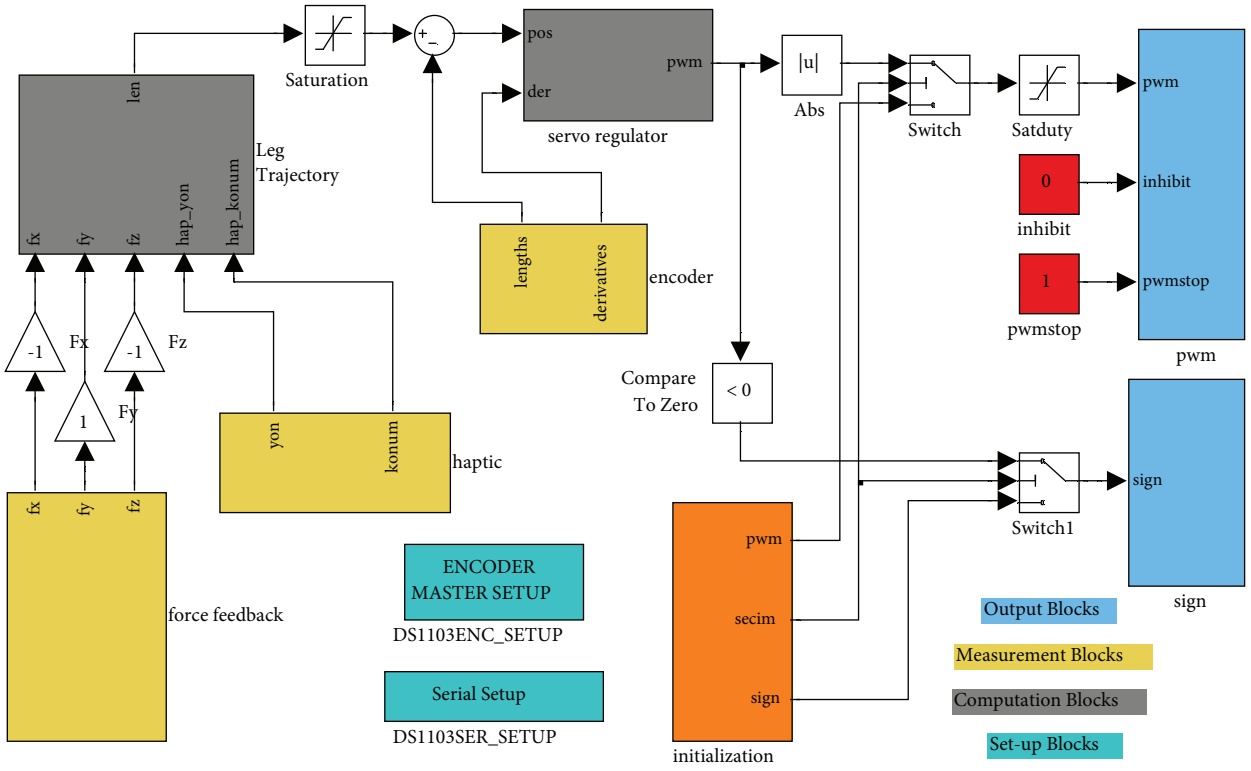

Figure 11. The ds1103 model of the fuzzy impedance/force controller.

The fuzzy impedance/force controller subsystem and force measurement subsystem are presented in Figures 12 and 13, respectively. The impedance filter, fuzzy controller with input/output scales, and integrator with threshold/reset control can be seen in Figure 12. The forces are measured, filtered, and converted to SI unit using analog-to-digital converters and sent to the force controller and haptic for force feedback in the force measurement subsystem shown in Figure 13.

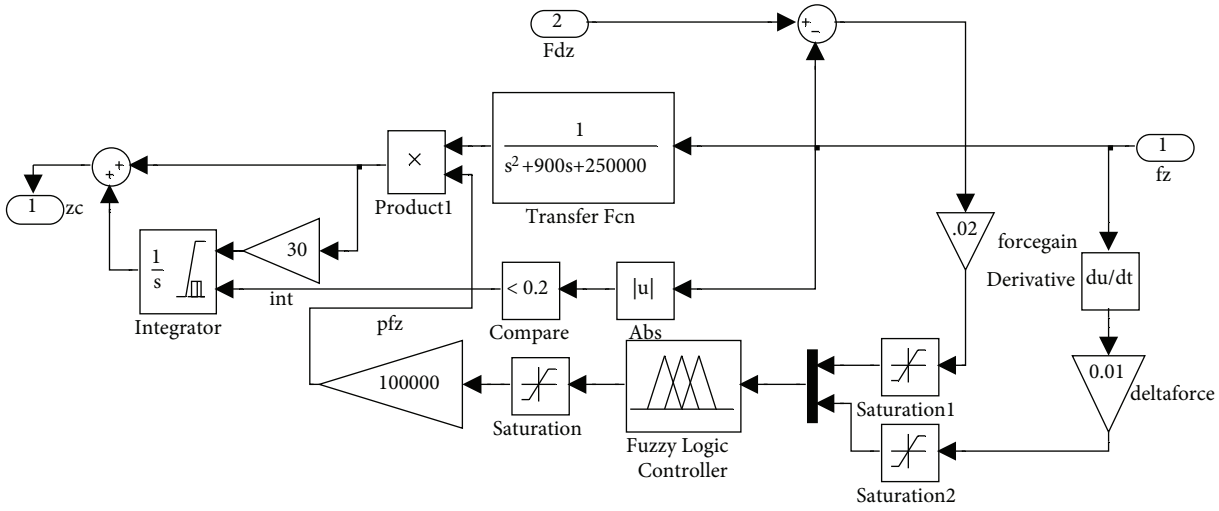

Figure 12. Fuzzy impedance/force controller subsystem.

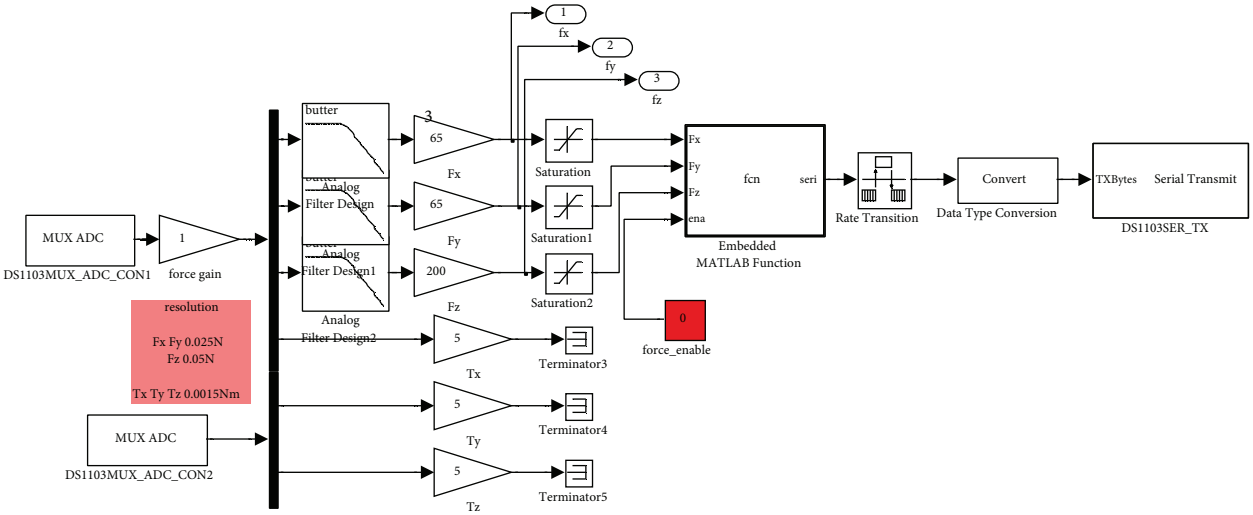

Figure 13. Force measurement subsystem.

Some of the real-time experimental results are given below. Figure 14 shows the position response of the SP guided by the haptic device in free space. The desired position and orientation inputs applied by the haptic in Cartesian space and actual robot behavior, which is computed offline using forward kinematics, are also shown in Figure 14. The position control of the robot is achieved in free space at up precision of 0.5 μm and 0.43 μ° in linear and rotational motions, respectively.

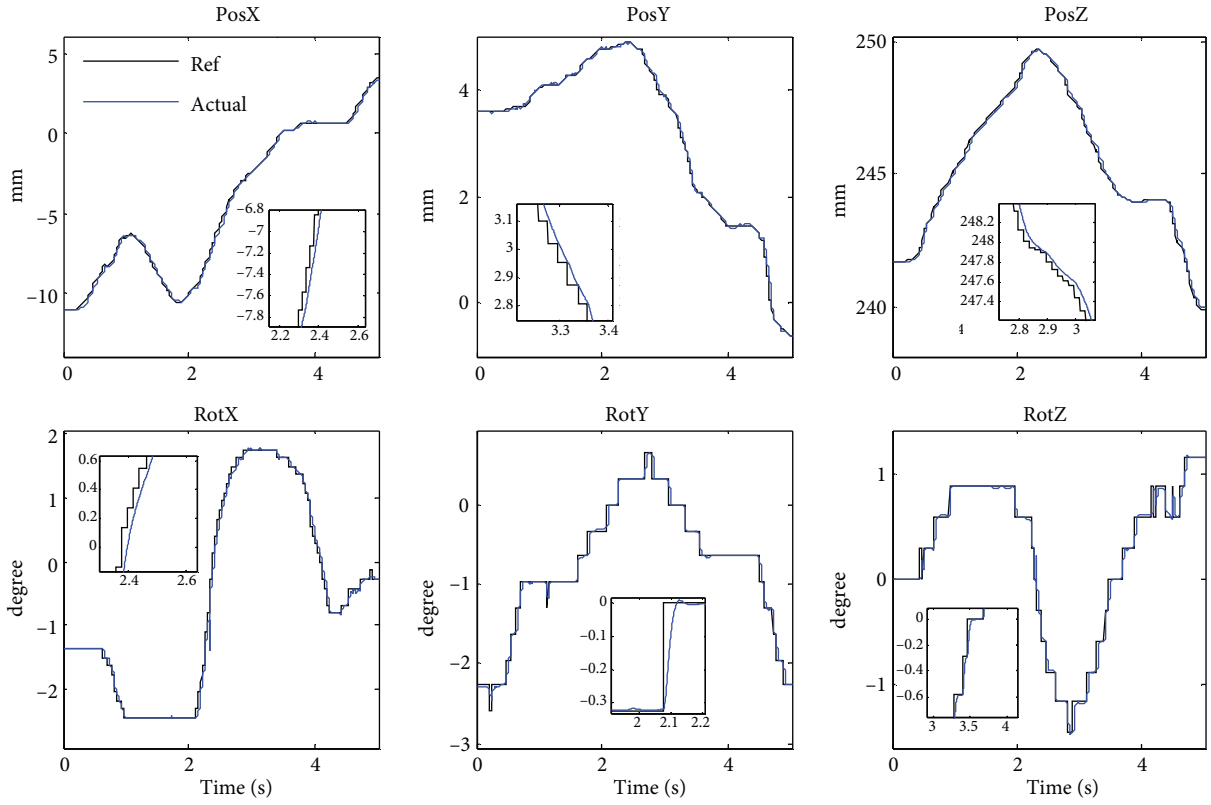

Figure 14. Position control of the SP with a haptic device in free space.

Interaction and force experiments are done after the positional experiments. Impedance and force control of the robot is dominant after any contact. Accordingly, system responses to a 5-N reference force and 11-mm reference position in the z-axis is shown in Figure 15. The reference and measured force, and reference and modified position by the fuzzy impedance/force controller are illustrated in Figures 14 and 15. The robot interacts with a sponge with a stiffness of 4700 N/m. A small overshoot and fast response for the interaction control and desired force control are obtained as designed.

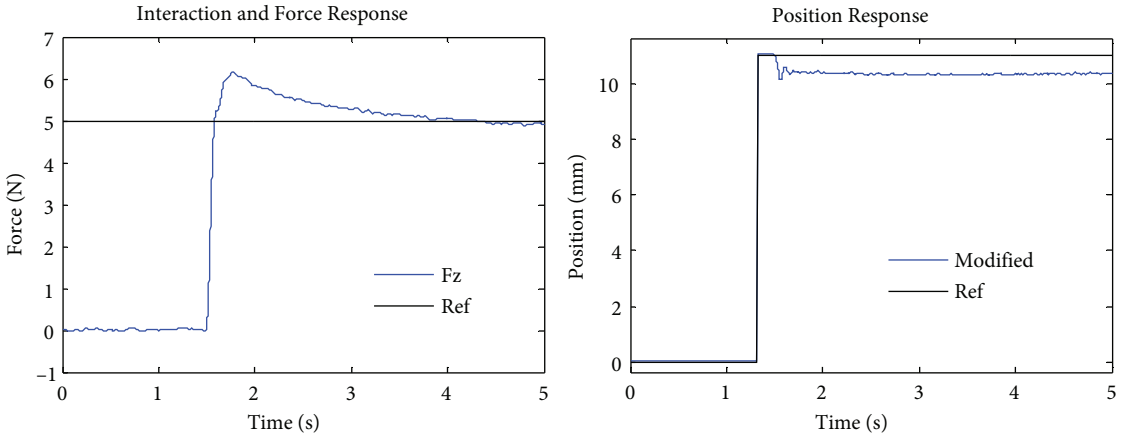

Figure 15. Impedance/force and robot position responses to the 5-N force and 11-mm position reference in the z-axis.

System responses to the 10-N force reference and 15-mm position reference in the z-axis are shown in Figure 16. As can be seen from the response, a similar desired response is obtained, despite the changes in the force and position reference.

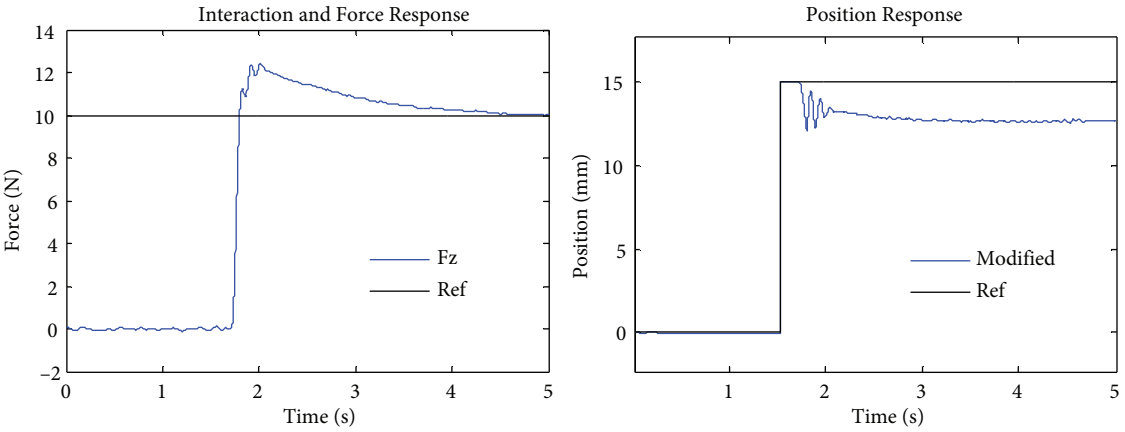

Figure 16. Impedance/force and robot position responses to the 10-N force and 15-mm position reference in the z-axis.

The robot can be brought to free space while it is in contact with an object and applying the desired force to the object. This situation is illustrated in Figure 17. The robot moves to the zero position in the z-axis, while the 10-N force is applied to the object.

The same experiments are carried out using different springs. In Figure 18, the system response is given under a 5-N force and 9-mm position reference in the z-axis with a spring that has 2300-N/m stiffness. The controller performs similar performances with different objects in contact.

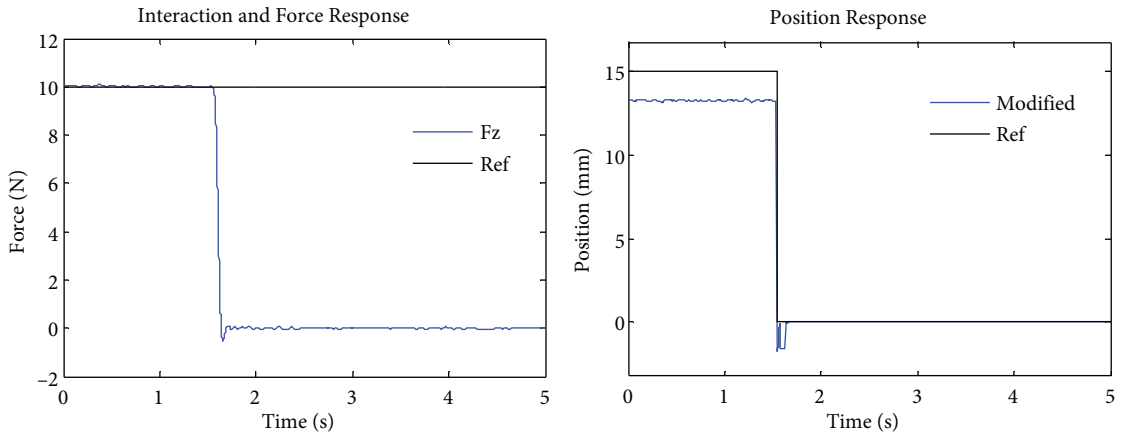

Figure 17. Reference position change under force control.

Finally, another condition is considered in Figure 19. The system response is obtained under an 8-N force and 15-mm position reference in the z-axis with a 5000-N/m spring.

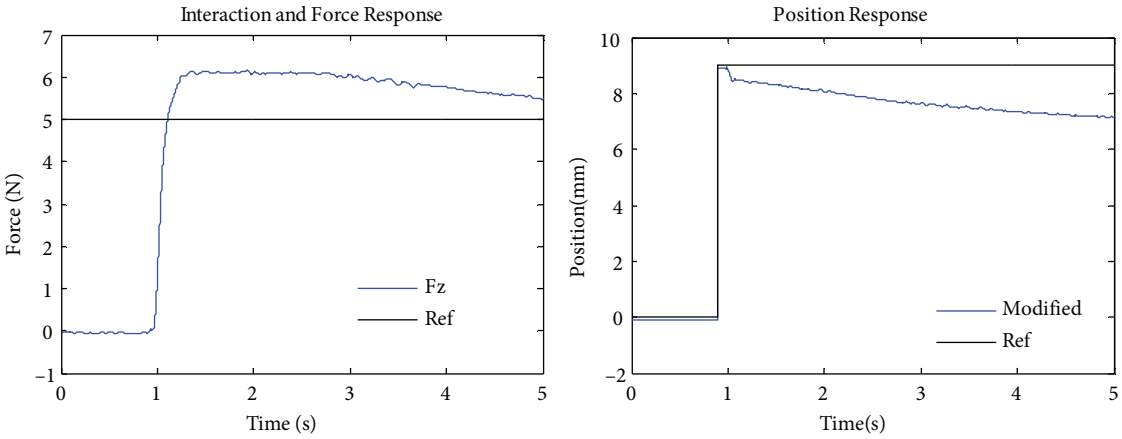

Figure 18. Interaction and force responses with a spring having stiffness of 2300 N/m, where Fd = 5 N and Zd = 9 mm.

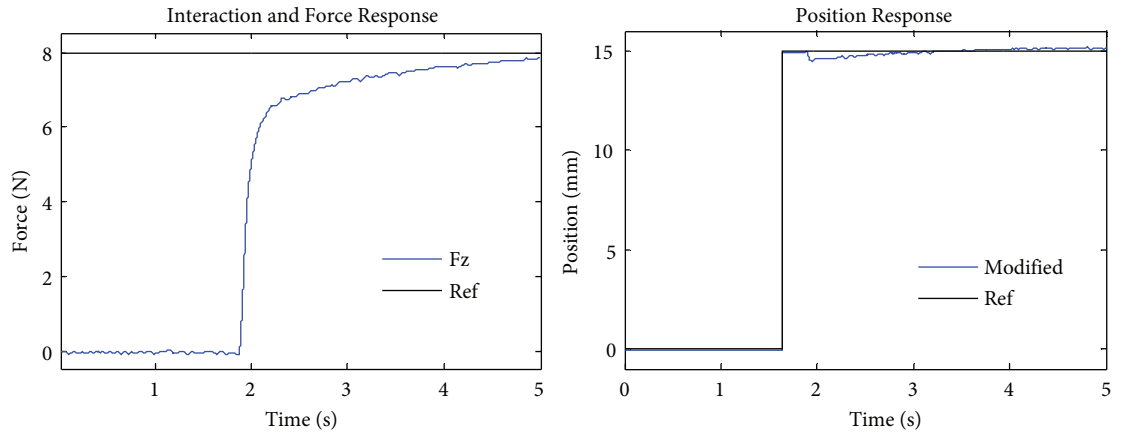

Figure 19. Interaction and force responses with a spring having stiffness of 5000 N/m, where Fd = 8 N, Zd = 15 mm.

7. Conclusion

In this study, a new controller is proposed for the impedance and force control of a 6-DOF SP. The impedance controller is designed as a second-order filter. The gain of this filter is adjusted using a fuzzy PID controller for the interaction and force control of a robot during contact with a surface. The kinematic and dynamic model of the SP are derived and simulated in Simulink. In order to show the effectiveness of the developed controller, several simulation and experiments are carried out. The proposed controller is embedded in a Dspace 1103 real-time controller. The experimental and simulation results show that the desired system performance is obtained with the proposed controller. The desired impedance force control is achieved in 0.3 s when the SP interacts with objects whose stiffness is between 2300 N/m and 5000 N/m.

Acknowledgment

The authors would like to thank the Scientific and Technological Research Council of Turkey (TÜBİTAK) for its financial support (Grant No. 107M148).

References

[1] I. Bonev, "The true origins of parallel robots", 06.04.2011, Available from: http://www.parallemic.org/Reviews/Review007.html.

[2] S. Kizir, Z. Bingul, Position Control and Trajectory Tracking of the Stewart Platform, Serial and Parallel Robot Manipulators - Kinematics, Dynamics, Control and Optimization, ISBN: 978-953-51-0437-7, InTech, 2012.

[3] O. Castillo, P. Melin, "Type-2 fuzzy logic: theory and applications", Studies in Fuzziness and Soft Computing, Vol. 223, 2008.

[4] V.E. Ömürlü, İ. Yıldız, "Self-tuning fuzzy PD-based stiffness controller of a 3 × 3 Stewart platform as a man-machine interface", Turkish Journal of Electrical Engineering & Computer Sciences, Vol. 19, pp. 743–753, 2011.

[5] N. Hogan, "Impedance control: An approach to manipulation: Part I-theory", Journal of Dynamic Systems, Measurement, and Control, Vol. 107, pp. 1–7, 1985.

[6] G. Zeng, A. Hemami, "An overview of robot force control", Robotica, Vol. 15, pp. 473–482, 1997.

[7] T. Yoshikawa, "Force control of robot manipulators", Proceedings of the IEEE International Conference on Robotics & Automation, pp. 220–226, 2000.

[8] D.E. Barkana, "Design and implementation of a control architecture for a robot-assisted orthopedic surgery", International Journal of Medical Robotics and Computer Assisted Surgery, Vol. 6, pp. 42–56, 2010.

[9] C. Yueyan, Z. Ji, W. Bidou, H. Shuang, "High-precision fuzzy impedance control algorithm and application in robotic arm", International Conference on Advanced Intelligent Mechatronics Monterey, Vol. 2, pp. 905–910, 2005.

[10] J. Seul, T.C. Hsia, R.G. Bonitz, "Force tracking impedance control of robot manipulators under unknown environment", IEEE Transactions on Control Systems Technology, Vol. 12, pp. 474–483, 2004.

[11] R.V. Patel, H.A. Talebi, J. Jayender, F. Shadpey, "A robust position and force control strategy for 7-DOF redundant manipulators", IEEE/ASME Transactions on Mechatronics, Vol. 14, pp. 575–589, 2009.

[12] I. Bonilla, E.J. Gonzalez-Galvan, C. Chavez-Olivares, M. Mendoza, A. Loredo-Flores, F. Reyes, B. Zhang, "A vision-based, impedance control strategy for industrial robot manipulators", IEEE Conference on Automation Science and Engineering, pp. 216–221, 2010.

[13] C.C. Cheah, D. Wang, "Learning impedance control for robotic manipulators", IEEE Transactions on Robotics and Automation, Vol. 14, pp. 452–465, 1998.

[14] M. Vukobratovic, D. Surdilovic, Y. Ekalo, D. Katic, Dynamics and Robust Control of Robot-Environment Interaction, Singapore, World Scientific Publishing, 2009.

[15] I. Davliakos, E. Papadopoulos, "Impedance model-based control for an electrohydraulic Stewart platform", European Journal of Control, Vol. 5, pp. 1–18, 2009.

[16] J. Lin, C.W. Chen, "Computer-aided-symbolic dynamic modeling for Stewart-platform manipulator", Robotica, Vol. 27, pp. 331–341, 2009.

[17] Z. Bingul, O. Karahan, Dynamic Modeling and Simulation of Stewart Platform, Serial and Parallel Robot Manipulators - Kinematics, Dynamics, Control and Optimization, ISBN: 978-953-51-0437-7, InTech, 2012.

[18] F. Almeida, A. Lopes, P. Abreu, Force-impedance control: a new control strategy of robotic manipulators, In: Kaynak O, Tosunoglu S, Marcelo Ang Jr (Eds.) Recent Advances in Mechatronics, Springer, Singapore, 1999.

[19] R.Z. Stanisic, Á.V. Fernández, "Adjusting the parameters of the mechanical impedance for velocity, impact and force control", Robotica, Vol. 30, pp. 583–597, 2012.